

## Double $K$ -shell ionization in the electron capture decay of $^{85}\text{Sr}$

G. Schupp

*Physics Department, University of Missouri-Columbia, Columbia, Missouri 65211*

H. J. Nagy

*Physics Department, Washburn University of Topeka, Topeka, Kansas 66621*

(Received 19 December 1983)

The probability per  $K$  capture for double  $K$ -shell ionization in the electron capture decay of  $^{85}\text{Sr}$  has been studied by recording coincidences between  $\text{Rb } K$  x rays and  $\text{Rb } K\alpha$  x rays produced when the two  $K$ -shell vacancies are filled. The probability for this decay was found to be  $(6.0 \pm 0.5) \times 10^{-5}$ , which is a factor of  $0.64 \pm 0.05$  times the recent theoretical prediction by Suzuki and Law. The energy shift of the hypersatellite  $\text{Rb } K\alpha^H$  x ray was found to be  $385 \pm 28$  eV, in agreement with the calculation of Chen, Craseman, and Mark.

### I. INTRODUCTION

In electron capture (EC) decay, double  $K$ -shell ionization occurs when one  $K$  electron is captured and the other is ejected from the atom [shakeoff (SO)] or is excited to an unoccupied bound state [shakeup (SU)]. The SO and SU processes for the  $K$  shell occur with a total probability of order  $10^{-4}$  per  $K$  capture owing to the somewhat compensating effects of the sudden reduction in nuclear charge and the sudden disappearance of the electron-electron Coulomb interaction. The filling of the empty  $K$  shell is accompanied by the nearly simultaneous ( $\sim 10^{-15}$  s) emission of either two  $K$  x rays, two Auger electrons, or by one  $K$  x ray and one Auger electron. Reviews of the phenomenon have been presented by Freedman,<sup>1</sup> Walen and Briancon,<sup>2</sup> and by Bambynek *et al.*<sup>3</sup>

Theoretical calculations for the probability per  $K$  capture for double  $K$ -shell ionization,  $P_{KK}$ , were first performed by Primakoff and Porter<sup>4</sup> in 1953. Further calculations were presented by several authors<sup>5-9</sup> in the late 1960's and early 1970's. In the latest theory, Suzuki and Law (SL) (Ref. 10) use Dirac-Fock-Slater wave functions and self-consistent-field calculations in their description of the initial and final electron states. A noteworthy result of their calculations is that the probability for shakeup,  $P_{KK}^{\text{SU}}$ , is much less than the probability for shakeoff,  $P_{KK}^{\text{SO}}$ , giving  $P_{KK} \cong P_{KK}^{\text{SO}}$ .

Experimental values for  $P_{KK}$  are generally deduced from coincidence measurements between the  $K$  x rays emitted when the double vacancy is filled. The first x ray, a  $K$  hypersatellite ( $K^H$ ,  $1s^{-2} \rightarrow 1s^{-1}2p^{-1}$ ), and the second x ray, a  $K$  satellite ( $K^S$ ,  $1s^{-1}2p^{-1} \rightarrow 2p^{-2}$ ), are shifted to higher energy with respect to normal  $K$  x rays because of the additional electron vacancy. The  $K^H$  shift has been recently calculated by Chen, Craseman, and Mark<sup>11</sup> and is substantially greater than the  $K^S$  shift. Resolution of the  $K^H$  x rays from the  $K^S$  and normal  $K$  x rays is possible with modern detectors and allows trustworthy values of  $P_{KK}$  to be determined for decays which may be complicated by  $K$  x rays from EC in coincidence with  $K$  x rays from internal conversion or low energy Compton photons.

Agreement between experiment and theory, even with

the latest techniques available to both, is not as good as might be expected. The average  $P_{KK}$  value for the decay branches in  $^{65}\text{Zn}$  was recently measured<sup>12</sup> to be a factor of  $1.44 \pm 0.13$  times the SL theory, while  $P_{KK}$  for  $^{165}\text{Er}$  and  $^{181}\text{W}$  were recently measured<sup>13</sup> to be factors of  $0.48 \pm 0.16$  and  $1.75 \pm 0.44$ , respectively, times the SL theory. When referring to the SL theory, we use their local density approximation values denoted by  $P(\text{LDA})$  in Ref. 10. Other comparisons between theory and experiment show that no one theory gives overall agreement. (See Tables I and III of Ref. 10 and Fig. 4 of Ref. 13.) A smooth trend suggests, however, that the theoretical values do not decrease with increasing  $Z$  as fast as the experimental values do, whereas the  $^{181}\text{W}$  result may indicate a problem for decay energies near threshold.

The present experiment on  $^{85}\text{Sr}$  was undertaken to help give a better data base for delineating the apparent discrepancies between experiment and theory. As seen from the decay scheme<sup>14</sup> of  $^{85}\text{Sr}$  shown in Fig. 1, the EC proceeds almost completely through the 0.514-MeV level

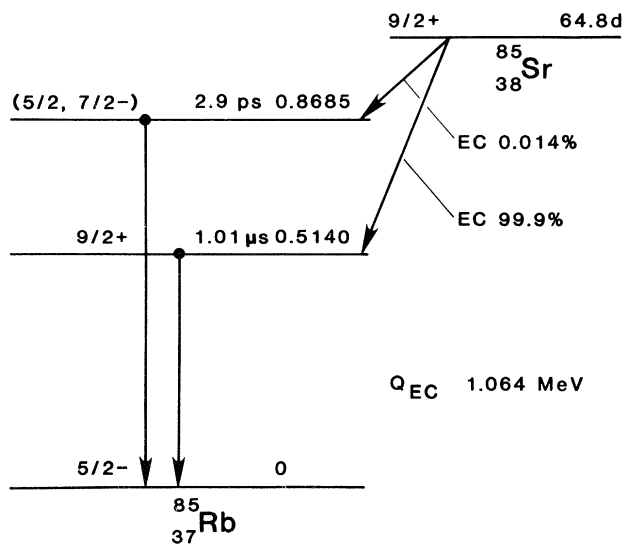


FIG. 1. Decay scheme of  $^{85}\text{Sr}$ .

which has a half-life of 1.01  $\mu$ s. This half-life eliminates the double  $K$ -shell vacancies that could in principle be formed by the EC followed by internal conversion of the 0.514-MeV transition if the nuclear level had an extremely short half-life ( $\sim 10^{-15}$  s). Even assuming an electronic half-life for the level at 0.868 MeV, the decay fraction to this level of  $1.4 \times 10^{-4}$  and the  $K$ -shell internal conversion coefficient,  $\alpha_K(0.868)$ , for the 0.868 MeV transition<sup>14</sup> of  $0.8 \times 10^{-3}$  give a probability for double  $K$ -shell ionization of near  $10^{-7}$ , which is at least a factor of  $10^2$  smaller than could be expected for  $P_{KK}$ . Similarly, the number of  $K\alpha^H$  x rays which could be produced by shakeoff accompanying the internal conversion of the 0.514-MeV transition is at least smaller than  $P_{KK}$  by the factor  $\alpha_K(0.514)$  which has been measured to be 0.0059.<sup>14</sup> With these fundamental difficulties for the experiment discounted, the 64.8 d half-life and 13.37-keV Rb  $K\alpha$  x rays makes the long counting times and x-ray detection rather straightforward. Complications in determining the coincidence efficiency caused by the 1.01  $\mu$ s half-life will be discussed later.

## II. EXPERIMENTAL PROCEDURES

### A. Electronic circuitry and detectors

In this investigation  $P_{KK}$  was deduced from the coincidences recorded between the Rb  $K\alpha^H$  and  $K^S$  x rays ( $K\alpha^H K^S$  coincidences). The schematic diagram of detectors and circuits used for these measurements is shown in Fig. 2. While both  $K\alpha^H$  and  $K^S$  x rays were detected in both detectors, the  $K\alpha^H$  x rays were resolved only by the Si(Li) detector; hence the  $K^S$  x rays in coincidence were detected by the NaI(Tl) x-ray detector. This arrangement

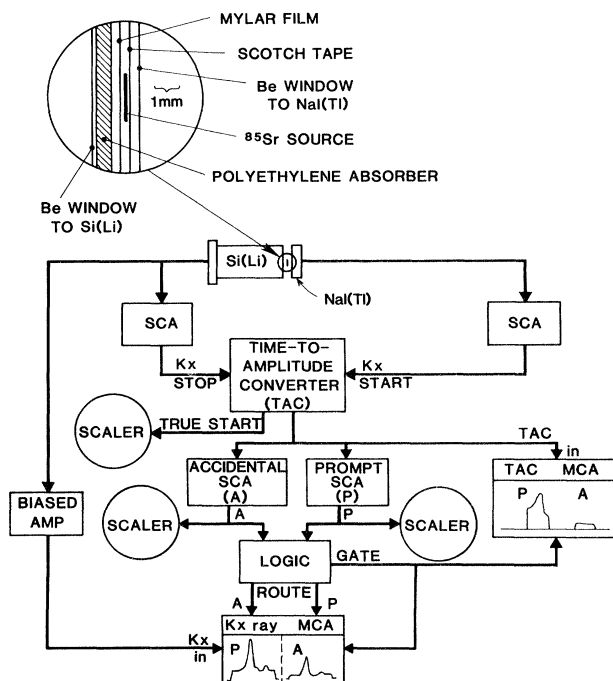


FIG. 2. Schematic diagram of detectors and circuits. Preamplifiers, amplifiers, and delay circuits have been omitted for simplicity.

is very similar to that used in recent investigations<sup>12,15,16</sup> of shakeoff in both position and EC decays. The main electronic circuitry difference between this and the earlier investigations was associated with the recording of the time-to-amplitude converter (TAC) spectra. For the earlier investigations free or ungated TAC spectra were recorded during the entire duration of each run with periodic checks taken on the positions and widths of the prompt and accidental single-channel analyzer (SCA) windows. For this investigation the TAC spectra recorded were alternated (about every two days) between a free or ungated mode and a mode in which the TAC spectra were gated by the prompt and accidental SCA's. Figure 3 shows the resultant TAC spectra for one run and will be discussed in detail in Sec. III.

The Si(Li) x-ray detector was an Ortec 7000 series with a 4 mm diameter, a 4.2 mm sensitive depth, an 0.008 mm Be window, a 10 mm window to detector distance, and a peak width (FWHM) of 160 eV at 5.9 keV. The NaI(Tl) detector had a 5.1 cm diameter, a thickness of 3 mm, and a 0.13 mm Be window.

### B. $^{85}\text{Sr}$ source

The  $^{85}\text{Sr}$  activity used in this study was purchased from New England Nuclear Corporation and no evidence for complicating impurities was seen in a long run with a well-shielded Ge detector system. Two separate sources were used during the course of the experiment. Source *A* was used for two runs and had activities of 0.133 and 0.065  $\mu$ Ci at the start of its runs, while source *B* had a strength of 0.049  $\mu$ Ci at the start of its run. Each source

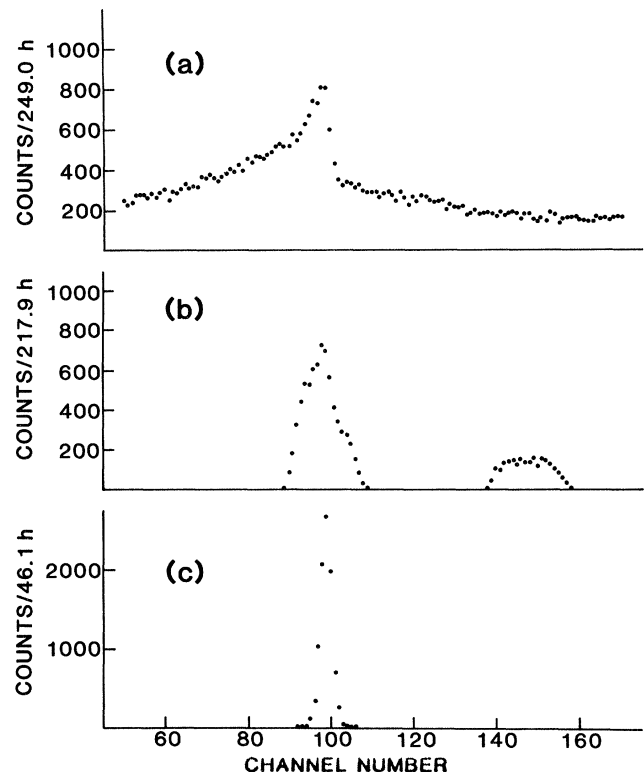


FIG. 3. TAC spectra. (a) Ungated spectrum. (b) Gated spectrum. (c) Prompt spectrum recorded using a  $^{75}\text{Se}$  source.

was prepared by evaporating drops of active solution onto a 0.01 mm thick Mylar backing. After drying, the sources were covered with Scotch Brand tape and placed between the detectors in a close geometry.

### III. DATA ANALYSES

Since the EC decay can be taken to be 100% to the 0.514-MeV level as argued earlier, the total number of  $K\alpha^H K^S$  coincidences recorded during a run,  $N(K\alpha^H K^S)$ , is given by

$$N(K\alpha^H K^S) = N_0 (K/T) P_{KK} \omega_K^S (aE)_{\text{NaI}}^S \times \omega_K^H (aE)_{\text{Si}}^H (K\alpha/K_T)^H E_T, \quad (1)$$

where  $N_0$  is the total number of decays during the run,  $K/T$  is the  $K$ -shell-to-total capture ratio for the EC to the 0.514-MeV level,  $P_{KK}$  is the probability for double  $K$ -shell ionization per  $K$  capture,  $\omega_K^S$  and  $\omega_K^H$  are the  $K$ -shell fluorescence yields for the Rb  $K^S$  and  $K\alpha^H$  x rays,  $(aE)_{\text{NaI}}^S$  and  $(aE)_{\text{Si}}^H$  are the products of absorption factors ( $a$ ) and total detection efficiencies ( $E$ ) for the Rb  $K^S$  x rays in the NaI(Tl) detector and for the  $K\alpha^H$  x rays in the Si(Li) detector,  $(K\alpha/K_T)^H$  is the  $K\alpha^H$  fraction of all  $K^H$  x rays, and  $E_T$  is the TAC coincidence efficiency. The very slight variation in  $P_{KK}$  and  $K/T$  for the 0.014% branch to the 0.868-MeV level was neglected in this study. The total number of Rb  $K$  x rays detected in the NaI(Tl) x ray detector during the same run,  $N(K)$ , is given by

$$N(K) = N_0 (K/T) \omega_K (aE)_{\text{NaI}}, \quad (2)$$

where  $\omega_K$  is the  $K$ -shell fluorescence yield for normal Rb  $K$  x rays and  $(aE)_{\text{NaI}}$  is the product of the absorption and total efficiency factors for the normal  $K$  x rays in the NaI(Tl) detector. The very low intensity contribution to the  $K$  x rays by internal conversion as well as by the  $K^S$  and  $K^H$  x rays has been neglected in this expression. Assuming  $\omega_K^S = \omega_K^H = \omega_K$  and that  $(aE)_{\text{NaI}}^S = (aE)_{\text{NaI}}$ , the ratio of Eq. (1) to Eq. (2) gives

$$P_{KK} = \left[ \frac{N(K\alpha^H K^S)}{N(K)} \right] \frac{1}{\omega_K (K\alpha/K_T)^H} \frac{1}{(aE)_{\text{Si}}^H} \frac{1}{E_T}. \quad (3)$$

The  $(aE)_{\text{Si}}^H$  factor in Eq. (3) was taken to be the same as  $(aE)_{\text{Si}}$  and was determined from singles runs. Neglecting  $K$  x rays produced by internal conversion or shakeoff effects, the number of  $K\alpha$  x rays observed in a singles run with a Si(Li) detector,  $N(K\alpha)$ , is given by

$$N(K\alpha) = N_0 (K/T) \omega_K (K\alpha/K_T) (aE)_{\text{Si}}, \quad (4)$$

where the number of decays  $N_0$  comes from the source strength determinations made with a well-calibrated Ge system. Experience with this system in earlier investigations where auxiliary coincidence runs could eliminate the need to know  $N_0$  independently has shown that the uncertainty in  $N_0$  is about 3%. For the predominant EC to the 0.514-MeV level, the  $K/T$  ratio was taken to be 0.894 and a value of 0.669 (Ref. 14) was used for  $\omega_K$ .

The  $N(K\alpha^H K^S)$  term of Eq. (3) was determined from least-squares computer fits to the  $K\alpha$ - $K\alpha^H$  region of both prompt and true coincidence spectra recorded with the Si(Li) detector. For a given run the true coincidence spec-

trum was obtained by subtraction of the computer fitted accidental spectrum from the actual prompt spectrum. The  $K\alpha$  region of the accidental spectrum was first fit with the sum of a modified Gaussian distribution of the form used by Jorch and Campbell<sup>17</sup> and a constant continuum. The  $K\alpha$ - $K\alpha^H$  region of the true coincidence spectrum was then fit with the sum of two modified Gaussian distributions, one for the main  $K\alpha$  peak and the other for the  $K\alpha^H$  peak, along with a constant continuum. The same shape parameters determined for the modified Gaussian  $K\alpha$  peak were used for the  $K\alpha^H$  peak. Values for  $N(K\alpha^H K^S)$  determined from computer fits directly to the prompt coincidence spectra before subtraction of the accidental coincidences were essentially the same as from the true spectra and showed how insensitive the  $P_{KK}$  determination was to experimental detail not represented in Eq. (3).

For normal Rb x rays  $(K\alpha/K_T) = 0.85$ .<sup>14</sup> Åberg *et al.*<sup>18</sup> have pointed out, however, that the ratio of  $K\alpha_1^H$  to  $K\alpha_2^H$  decreases considerably at low  $Z$ . Normal Rb  $K$  x rays have a value of 1.93 for this ratio, whereas Åberg *et al.* have estimated  $(K\alpha_1/K\alpha_2)^H$  to be 0.7. Assuming only the  $K\alpha_1^H$  transition to be suppressed yields  $(K\alpha/K_T)^H = 0.77$ . For this study an intermediate value of  $(K\alpha/K_T)^H = 0.81 \pm 0.04$  was used in Eq. (3).

Figure 3 shows typical TAC spectra taken during the course of this investigation. Curve (a) shows a free or ungated spectrum highlighted by exponentials resulting from the 1.01  $\mu$ s half-life of the 0.514-MeV level. Starting at the peak, the exponential decay to higher channels is caused by very low intensity Compton photons from the 0.514-MeV gamma ray in the Si(Li) detector in delayed coincidence with EC x rays seen by the NaI(Tl) detector. This situation is just reversed when going from the peak to lower channels where the more intense exponential distribution in this case comes from the fact that the NaI(Tl) detector has relatively more Compton photons from the 0.514-MeV gamma ray than the Si(Li) detector. Although these contributions lead to true coincidences, they do not lead to hypersatellite coincidences as was argued earlier. The "peak" seen in this upper curve includes the desired  $K\alpha^H K^S$  coincidences but is primarily due to internal bremsstrahlung accompanying  $K$  EC. The middle curve (b) shows the TAC spectrum gated by the prompt and accidental SCA's set with windows of 0.6  $\mu$ s. From this curve it is not clear how broad the prompt peak is and hence the bottom curve (c) was run in an auxiliary experiment using a <sup>75</sup>Se source. This source decays by EC to <sup>75</sup>As giving many possibilities for coincidences with  $K\alpha$  x rays at 10.5 keV compared to the 13.4-keV Rb  $K\alpha$  x rays. The prompt peak seen in the bottom curve was obtained simply by replacing the <sup>85</sup>Sr source with <sup>75</sup>Se. No gain or window adjustments were needed since the x rays already fell within the SCA windows set on the Si(Li) and NaI(Tl) spectra. When analyzing all of the coincidence runs, a value of  $0.97 \pm 0.03$  was used for the TAC efficiency,  $E_T$ , which is simply the fraction of the desired coincidences falling within the prompt window on the TAC spectrum.

Since the  $K$  x rays in the NaI(Tl) x-ray spectrum ride on the low-intensity Compton continuum from the 0.514-MeV gamma rays mentioned above, the NaI(Tl) spectrum

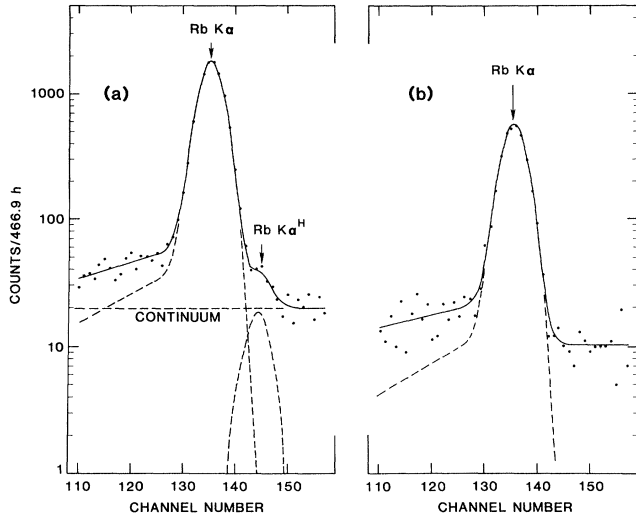


FIG. 4. (a) Prompt coincidence spectrum in the  $K\alpha$ - $K\alpha^H$  region. The solid curve gives the overall fit to the data, whereas the dashed curves give the components of this fit, the  $K\alpha$  x-ray peak, the  $K\alpha^H$  x-ray peak, and the constant continuum. (b) Accidental coincidence spectrum in the  $K\alpha$ - $K\alpha^H$  region.

was carefully analyzed to determine the fraction of total counts from the SCA used to start the TAC which was attributable to the  $K$  x rays. This fraction was found to be  $0.98 \pm 0.01$  for the experimental arrangement used and when multiplied by the counts recorded on the true starts scaler gave  $N(K)$  in Eq. (3).

#### IV. RESULTS

Figure 4 shows the (a) prompt and (b) accidental coincidences recorded in the Rb  $K\alpha$  region of the Si(Li) detector for the 466.9 h run. As an experimental variation, the gain and off-set adjustments for these spectra were set to give a FWHM of 5.2 channels compared to 8.5 and 8.8 channels for the first two runs, respectively. Figure 4(a) also shows the shape function determined from the accidental spectrum fitted to the  $K\alpha$  and  $K\alpha^H$  regions along with the constant continuum. The contribution due to the hypersatellite component was completely insensitive in all the runs as to whether the least-squares fitting was done on the prompt or true coincidence spectra. The approximate factor of 3 between the prompt and accidental Rb  $K\alpha$  x rays is, of course, the same as the ratio of the counts seen in the gated TAC spectrum of Fig. 3(b). Although the accidental window may include some delayed true coincidences, they do not lead to  $K\alpha^H$  x rays and hence do not affect the  $P_{KK}$  determination. While the principal

contribution to the  $K\alpha$  coincidences can be seen from the TAC spectrum in Fig. 3(a) to be due to delayed coincidences between the low-energy Compton photons from the 0.514-MeV gamma rays and the  $K\alpha$  x rays from EC, these coincidences do not lead to  $K\alpha^H$  x rays as argued earlier.

Table I shows the remaining data needed to calculate  $P_{KK}$  from Eq. (3) for each run and the results of those calculations. The uncertainties on the individual and average  $P_{KK}$  values were based on a statistical contribution from the total number of  $K\alpha^H$  coincidences represented folded with independent systematic uncertainties of 3% for the TAC efficiency, 3% for the  $(aE)_{Si}$  factors, and 5% for the  $(K\alpha/K_T)^H$  ratio. The average  $P_{KK}$  value of  $(6.0 \pm 0.5) \times 10^{-5}$  is a factor of  $0.64 \pm 0.05$  times the SL theoretical value<sup>19</sup> of  $9.38 \times 10^{-5}$ .

The energy differences,

$$\Delta E = E(K\alpha^H) - E(K\alpha),$$

found for the three runs and the average value are given in Table I. The  $E(K\alpha)$  value of 13.375 keV used to obtain  $\Delta E$  was taken as the weighted average of  $E(K\alpha_1)$  and  $E(K\alpha_2)$ .<sup>14</sup> The uncertainties for the individual energy differences were estimated to be about 7% from the fitting variations. This value is consistent with that obtained from deviations about the mean, but we felt that the energy resolution of the hypersatellite did not support a smaller uncertainty for the averaged value. This value is in good agreement with a value of approximately 395 eV predicted by Chen *et al.*<sup>11</sup>

#### V. DISCUSSION

In discussing these results, we would like to try to bring the comparisons between experiment and theory up-to-date. Unfortunately, the experimental results of van Eijk *et al.*<sup>13</sup> on <sup>165</sup>Er and <sup>181</sup>W were published shortly after the SL theory<sup>10</sup> and neither included communications with the other. In addition, our paper<sup>12</sup> on <sup>65</sup>Zn included comparisons with the SL theory but was in press too early to include the van Eijk results. In the comparisons with theories given below, we have arbitrarily included only experimental results beginning with Briand *et al.*<sup>20</sup> in 1971. In the case of <sup>109</sup>Cd, only the most recent measurement by van Eijk *et al.*<sup>21</sup> was used, while the earlier results by van Eijk and Wijnherts<sup>22</sup> and by Nagy *et al.*<sup>23</sup> were not included.

The sensitivity of the SL theory to decay energy was presented in Table II of Ref. 12 for <sup>65</sup>Zn and showed  $P_{KK}^{SO}$  values in the local density approximation (LDA) to be  $1.40 \times 10^{-4}$  and  $1.71 \times 10^{-4}$  for  $E - B_K$  energies of 227.4 and 1342.9 keV, and  $(E - B_K)/B_K$  ratios of 25.3 and

TABLE I. Data necessary for the calculation of  $P_{KK}$  from Eq. (3);  $P_{KK}$  and  $\Delta E$  values.

Run	Source	Time (h)	$N(K\alpha^H K^S)$	$N(K)$ ( $\times 10^{-6}$ )	$(aE)_{Si}$ ( $\times 10^3$ )	$P_{KK}$ ( $\times 10^5$ )	$\Delta E$ (eV)
I	A	379.6	$104.5 \pm 10.2$	544.8	$6.5 \pm 0.2$	$5.7 \pm 0.7$	$366 \pm 26$
II	B	901.3	$70.5 \pm 8.4$	328.9	$7.0 \pm 0.2$	$5.9 \pm 0.8$	$412 \pm 30$
III	A	466.9	$110.2 \pm 10.5$	513.9	$6.4 \pm 0.2$	$6.4 \pm 0.8$	$378 \pm 27$
Average						$6.0 \pm 0.5$	$385 \pm 28$

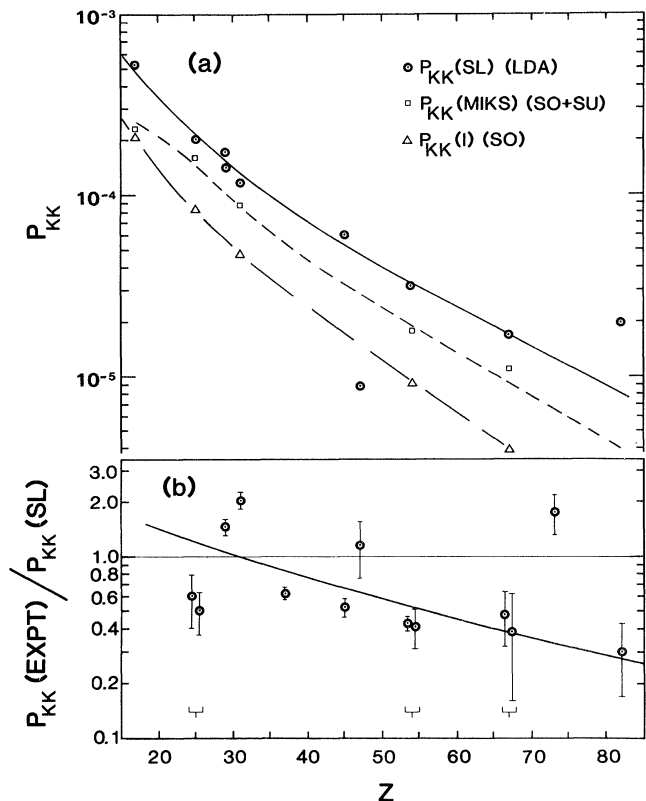


FIG. 5. (a) Values for  $P_{KK}$  calculated from the theories indicated. (b) Ratios of experimental values of  $P_{KK}$  to the theoretical values of SL. Isotopes for which experimental values are shown are, in order of increasing  $Z$ ,  $^{55}\text{Fe}$  (Refs. 24 and 25),  $^{65}\text{Zn}$  (Ref. 12),  $^{71}\text{Ge}$  (Ref. 20),  $^{85}\text{Sr}$  (the present result),  $^{103}\text{Pd}$  (Ref. 26),  $^{109}\text{Cd}$  (Ref. 21),  $^{131}\text{Cs}$  (Refs. 27 and 28),  $^{165}\text{Er}$  (Refs. 13 and 27),  $^{181}\text{W}$  (Ref. 13), and  $^{207}\text{Bi}$  (Ref. 29). All results are plotted at the  $Z$  of the daughter atom. The smoothed curves are drawn only to aid the eye.

149.5, respectively, where  $E$  is the decay scheme transition energy and  $B_K$  is the  $K$ -shell binding energy of the daughter atom. This result shows that even at energies with  $(E - B_K)/B_K > 10$ , care should be exercised when estimating theoretical values from  $Z$  interpolations. Looking at the values calculated from the SL theory,  $P_{KK}(\text{SL})$ ,

plotted vs  $Z$  of the daughter atoms in Fig. 5(a), one sees a rather smooth dependence. The difference in the calculated values for  $^{65}\text{Zn}$  discussed above are seen to be rather unimportant with respect to the smooth curve when compared to the differences seen for  $^{109}\text{Cd}$ ,  $^{181}\text{W}$ , and  $^{207}\text{Bi}$ . The  $^{109}\text{Cd}$  decay has an  $(E - B_K)/B_K$  ratio of 2.68 which is seen to lower  $P_{KK}(\text{SL})$  by approximately a factor of 5 from the smooth curve. Similarly, the  $^{181}\text{W}$  decay has an  $(E - B_K)/B_K$  ratio of 1.79 and a  $P_{KK}(\text{SL})$  value<sup>19</sup> of  $0.137 \times 10^{-5}$  [not shown in Fig. 5(a)] which is approximately a factor of 10 below the smooth curve. The  $^{207}\text{Bi}$  case represents a forbidden decay and was discussed separately by SL. Also shown in Fig. 5(a) are smooth curves drawn through the theoretical values (including SU) of Mukoyama, Isozumi, Kitahara, and Shimizu<sup>9</sup> (MIKS),  $P_{KK}(\text{MIKS})$ , as well as the SO values calculated by Intemann,<sup>6</sup>  $P_{KK}(\text{I})$ .

Figure 5(b) shows the ratio  $P_{KK}(\text{expt})/P_{KK}(\text{SL})$  plotted vs  $Z$  for all of the recent experimental values. Neglecting the  $^{181}\text{W}$  data point, the smooth trend seen in Fig. 5(b) for the theoretical values of  $P_{KK}$  to be too small at low  $Z$  and too large at high  $Z$  seems to be real, although more experimental values at low  $Z$  would be helpful contributions. The comparison between experiment and theory for the  $^{181}\text{W}$  decay indicates another type of discrepancy for decay energies near threshold. Further investigations aimed at this aspect of shakeoff phenomena appear to be called for. When the  $P_{KK}(\text{expt})/P_{KK}(\text{MIKS})$  and  $P_{KK}(\text{expt})/P_{KK}(\text{I})$  ratios are plotted vs  $Z$ , similar trends are seen although these theories have been evaluated for only four of the experiments shown in Fig. 5(b). While theoretical values can be reasonably well interpolated for the  $^{65}\text{Zn}$ ,  $^{85}\text{Sr}$ , and  $^{103}\text{Pd}$  cases to yield trends, the  $^{181}\text{W}$ ,  $^{109}\text{Cd}$ , and  $^{207}\text{Bi}$  values represent important tests for these theories which have not been calculated. With so many of the  $P_{KK}(\text{MIKS})$  and  $P_{KK}(\text{I})$  values missing, definitive statements cannot be made about the theoretical description of the  $P_{KK}$  process. However, the  $Z$  dependence of Intemann and the overall magnitude of MIKS do appear to be more in agreement with the later experimental results than the SL theory.

We would like to thank the University of Missouri Research Reactor facility and staff for preparing and calibrating the sources used, and Dr. Law and Dr. Suzuki for supplying the latest  $P_{KK}(\text{SL})$  values for  $^{85}\text{Sr}$  and  $^{181}\text{W}$ .

<sup>1</sup>M. S. Freedman, *Annu. Rev. Nucl. Sci.* **24**, 209 (1974).

<sup>2</sup>R. J. Walen and Ch. Briancon, in *Atomic Inner Shell Processes*, edited by B. Craseman (Academic, New York, 1975), Vol. 1, p. 233.

<sup>3</sup>W. Bambynek, H. Behrens, M. H. Chen, B. Craseman, M. L. Fitzpatrick, K. W. D. Ledingham, H. Genz, M. Mutterer, and R. L. Intemann, *Rev. Mod. Phys.* **49**, 77 (1977).

<sup>4</sup>H. Primakoff and F. T. Porter, *Phys. Rev.* **89**, 930 (1953).

<sup>5</sup>R. L. Intemann and F. Pollock, *Phys. Rev.* **157**, 41 (1967).

<sup>6</sup>R. L. Intemann, *Phys. Rev.* **178**, 1543 (1969); **188**, 1963 (1969).

<sup>7</sup>P. Stephan and B. Craseman, *Phys. Rev.* **164**, 1509 (1967); P. Stephan, *ibid.* **186**, 1013 (1969); P. Stephan and B. Craseman, *Phys. Rev. C* **3**, 2495 (1971).

<sup>8</sup>J. Law and J. L. Campbell, *Nucl. Phys.* **A199**, 481 (1973).

<sup>9</sup>T. Mukoyama, Y. Isozumi, T. Kitahara, and S. Shimizu, *Phys. Rev. C* **8**, 1308 (1973).

<sup>10</sup>Akira Suzuki and J. Law, *Phys. Rev. C* **25**, 2722 (1982).

<sup>11</sup>M. H. Chen, B. Craseman, and H. Mark, *Phys. Rev. A* **25**, 391 (1982).

<sup>12</sup>H. J. Nagy and G. Schupp, *Phys. Rev. C* **27**, 2887 (1983).

<sup>13</sup>C. W. E. van Eijk, J. P. Wagenaar, F. Bergsma, and W. Lourens, *Phys. Rev. A* **26**, 2749 (1982).

<sup>14</sup>*Table of Isotopes*, 7th ed., edited by C. Michael Lederer and Virginia S. Shirley (Wiley, New York, 1978).

<sup>15</sup>S. K. Nha, G. Schupp, and H. J. Nagy, *Phys. Rev. C* **27**, 1276 (1983).

- <sup>16</sup>S. K. Nha, G. Schupp, and H. J. Nagy, *Phys. Rev. C* 27, 2879 (1983).
- <sup>17</sup>H. H. Jorch and J. L. Campbell, *Nucl. Instrum. Methods* 143, 551 (1977).
- <sup>18</sup>R. Åberg, J. P. Briand, A. P. Chevallier, A. Chetioui, J. P. Rozet, M. Tavernier, and A. Touati, *J. Phys. B* 9, 2815 (1976).
- <sup>19</sup>Akira Suzuki (private communication).
- <sup>20</sup>J. P. Briand, P. Chevallier, M. Tavernier, and J. P. Rozet, *Phys. Rev. Lett.* 27, 777 (1971).
- <sup>21</sup>C. W. E. van Eijk, J. Wijnhorst, and M. A. Popelier, *Phys. Rev. C* 19, 1049 (1979).
- <sup>22</sup>C. W. E. van Eijk and J. Wijnhorst, *Phys. Rev. C* 15, 1068 (1977).
- <sup>23</sup>H. J. Nagy, G. Schupp, and R. R. Hurst, *Phys. Rev. C* 11, 205 (1975).
- <sup>24</sup>J. P. Briand, P. Chevallier, A. Johnson, J. P. Rozet, M. Tavernier, and A. Touati, *Phys. Lett.* 49A, 51 (1974).
- <sup>25</sup>T. Kitahara and S. Shimizu, *Phys. Rev. C* 11, 920 (1975).
- <sup>26</sup>C. W. E. van Eijk, J. Wijnhorst, and M. A. Popelier, *Phys. Rev. A* 20, 1749 (1979).
- <sup>27</sup>H. J. Nagy, G. Schupp, and R. R. Hurst, *Phys. Rev. C* 6, 607 (1972).
- <sup>28</sup>Y. Isozumi, Ch. Briancon, and R. J. Walen, *Phys. Rev. C* 25, 3078 (1982).
- <sup>29</sup>J. P. Briand, J. P. Rozet, P. Chevallier, A. Chetioui, M. Tavernier, and A. Touati, *J. Phys. B* 13, 4751 (1980).